

# Phenylisoserine: A Versatile Amino Acid for the Construction of Novel $\beta$ -Peptide Structures

Irina A. Motorina,<sup>§</sup> Christiane Huel,<sup>‡</sup> Eric Quiniou,<sup>‡</sup> Joel Mispelter,<sup>‡</sup>  
Elisabeth Adjadj,<sup>\*,‡</sup> and David S. Grierson<sup>\*,†,§</sup>

Contribution from the UMR 176 CNRS, Laboratoire de Pharmacochimie, Institut Curie Section de Recherche, Batiment 110, Centre Universitaire, 91405 Orsay, France, the U350 INSERM, Laboratoire de Biophysique Moléculaire, Institut Curie Section de Recherche, Batiment 112, Centre Universitaire, 91405 Orsay, France, and the Institut de Chimie des Substances Naturelles CNRS, Ave de la Terrasse, 91198, Gif-sur-Yvette, France

Received July 21, 2000

**Abstract:** The *N*-Boc *O*-*tert*-butyldimethylsilyl-substituted hexa- $\beta$ -peptide methyl ester **18** was constructed from the *O*-TBS ether of (–)-(2*R*, 3*S*)-phenylisoserine. By NMR, it was determined that this homo  $\beta$ -peptide adopts a highly stable  $\beta$ -strand-type secondary structure in chloroform solution, which is stabilized by both hydrophobic interactions involving the OTBS methyl groups of residues *i* and *i* + 2, and inter-(five-membered)/intra (six-membered)-residue H-bonding interactions. These interactions are systematically repeated along the peptide chain and, thereby, operate in concert to stabilize the observed conformation of **18**.

## Introduction

Independent studies by Gellman and Seebach have clearly demonstrated that  $\beta$ -peptides composed of six or more residues can auto-organize to give remarkably stable  $\alpha$ -helix structures in solution (MeOH, pyridine).<sup>1–3</sup> For instance, the  $\beta$ -peptide **1** formed from *trans*-2-aminocyclohexane carboxylic acid organizes into a  $3_{14}$ -*M*  $\alpha$ -helix, and compound **2**, derived from the corresponding cyclopentane carboxylic acid, adopts a 12-helix in which the H-bonds are oriented in the opposite (or C-terminal) direction. Seebach showed that the acyclic  $\beta$ -peptide **3** forms a stable left-handed  $3_{14}$ -*M*  $\alpha$ -helix (pitch of 5 Å) and that the corresponding *R*-configuration  $\beta^2$ -peptide folds to give a right-handed  $3_{14}$  helical structure. However, this latter system appears to be less stable than  $\beta^3$ -peptides in solution. Most interesting,

the hepta  $\beta^{2,3}$ -disubstituted peptide **4** adopts a novel 12–10–12 helical conformation in which the central 10-membered hydrogen bonded ring resembles an  $\alpha$ -peptide turn-type structure.<sup>4</sup> Further incorporation of this turn motif into peptide **5** permits the C- and N-terminal  $\beta^{2,3}$ -unlike configuration fragments to adopt a  $\beta$ -sheet structure (evidenced by the occurrence of a large 10 Hz  $\beta^2$ H– $\beta^3$ H coupling constant).<sup>5</sup> Gellman has used L-proline–glycolic acid and dinipeptidic acid systems to create hairpin motifs (cf. **6**) in which the  $\beta^2, \beta^3$  hydrogens are also antiperiplanar.<sup>6</sup> First-generation examples of the three principle secondary structure elements ( $\alpha$ -helix,  $\beta$ -turn, and  $\beta$ -sheet) present in  $\alpha$ -proteins have, thus, been found. These systems bear a number of important analogies and differences to the corresponding  $\alpha$ -peptides/proteins substructures. Perhaps one of the most noticeable differences for the  $\alpha$ -helix conformation is that, whereas only six  $\beta$ -amino acid residues are necessary to form a stable  $\beta$ -peptide-based helix, approximately 15–20 residues are required to obtain a stable  $\alpha$ -peptide  $\alpha$ -helix. These unexpected results mark a point of departure for an exciting new field of investigation with the promise for new insights and perspectives into the problem of amino acid interactions and natural/unnatural protein folding,<sup>7</sup> as well as a wide range

<sup>†</sup> Institut de Chimie des Substances Naturelles CNRS.

<sup>‡</sup> Laboratoire de Biophysique Moléculaire.

<sup>§</sup> Laboratoire de Pharmacochimie.

(1) (a) Appella, D. H.; Christianson, L. A.; Karle, I. L.; Powell, D. R.; Gellman, S. H. *J. Am. Chem. Soc.* **1996**, *118*, 13071–13072. (b) Appella, D. H.; Christianson, L. A.; Klein, D. A.; Powell, D. R.; Huang, X.; Barchi, J. J.; Gellman, S. H. *Nature* **1997**, *387*, 381–384. (c) Appella, D. H.; Christianson, L. A.; Karle, I. L.; Powell, D. R.; Gellman, S. H. *J. Am. Chem. Soc.* **1999**, *121*, 6206–6212. (d) Appella, D. H.; Christianson, L. A.; Klein, D. A.; Richards, M. R.; Powell, D. R.; Gellman, S. H. *J. Am. Chem. Soc.* **1999**, *121*, 7574–7581. (e) Barchi, J. J.; Huang, X.; Appella, D. H.; Christianson, L. A.; Durell, S. R.; Gellman, S. H. *J. Am. Chem. Soc.* **2000**, *122*, 2711–2718.

(2) (a) Seebach, D.; Overhand, M.; Kühnle, F. N. M.; Martinioni, B.; Oberer, L.; Hommel, U.; Widmer, H. *Helv. Chim. Acta* **1996**, *79*, 913–941. (b) Seebach, D.; Ciceri, P.; Overhand, M.; Juan, B.; Rigo, D.; Oberer, L.; Hommel, U.; Amstutz, R.; Widmer, H. *Helv. Chim. Acta* **1996**, *79*, 2043–2066. (c) Hintermann, T.; Seebach, D. *Synlett* **1997**, 437–438. (d) Seebach, D.; Gademann, K.; Schreiber, J. V.; Matthews, J. L.; Hintermann, T.; Juan, B.; Oberer, L.; Hommel, U.; Widmer, H. *Helv. Chim. Acta* **1997**, *80*, 2033–2039. (e) Seebach, D.; Abele, S.; Gademann, K.; Guichard, G.; Hintermann, T.; Juan, B.; Matthews, J. L.; Schreiber, J. V. *Helv. Chim. Acta* **1998**, *81*, 932–982.

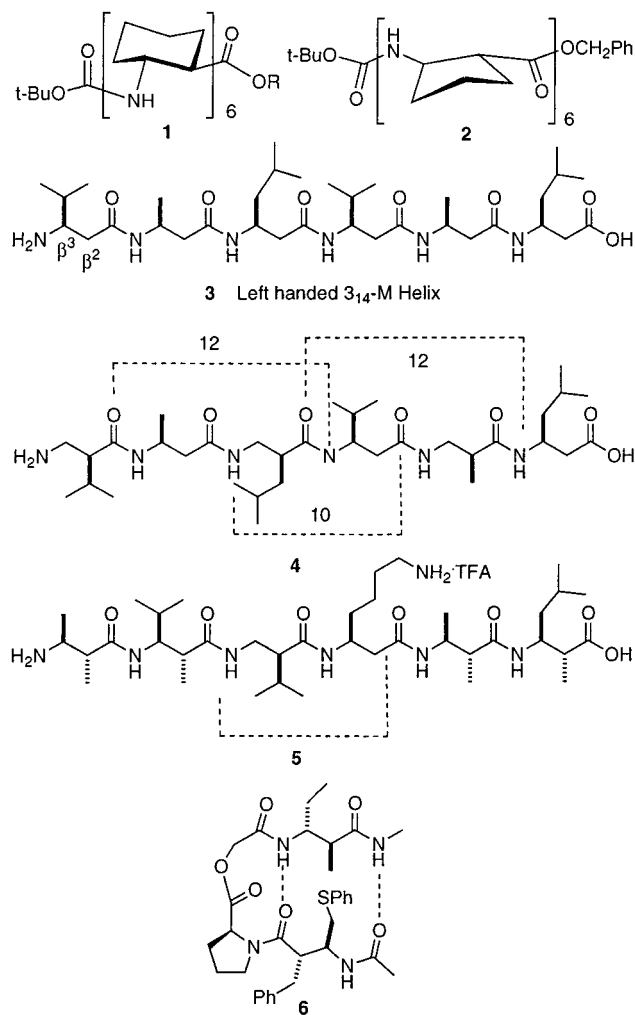
(3) For reviews, see: (a) Seebach, D.; Mathews, J. L. *J. Chem. Soc. Chem. Commun.* **1997**, 2015–2022. (b) Gellman, S. H. *Acc. Chem. Res.* **1998**, *31*, 173–180. (c) Gademann, K.; Hintermann, T.; Schreiber, J. V. *Curr. Med. Chem.* **1999**, *6*, 905–925. (d) DeGrado, W. F.; Schneider, J. P.; Hamuro, Y. *J. Peptide Res.* **1999**, *54*, 206–217.

(4) For a theoretical treatment of 14 and 12–10–12 helix structures; see: (a) Daura, X.; van Gunsteren, W. F.; Mark, A. E. *Proteins* **1999**, *34*, 269–280. (b) Daura, X.; Gademann, K.; Juan, B.; Seebach, D.; van Gunsteren, W. F.; Mark, A. E. *Angew. Chem., Int. Ed. Engl.* **1999**, *38*, 236–240. (c) Daura, X.; Juan, B.; Seebach, D.; van Gunsteren, W. F.; Mark, A. E. *J. Mol. Biol.* **1998**, *280*, 925–932. (d) Daura, X.; van Gunsteren, W. F.; Rigo, D.; Juan, B.; Seebach, D. *Chem. Eur. J.* **1997**, *3*, 1410–1417. (e) Wu, Y.-D.; Wang, D.-P. *J. Am. Chem. Soc.* **1998**, *120*, 13485–13493. (f) Wu, Y.-D.; Wang, D.-P. *J. Am. Chem. Soc.* **1999**, *121*, 9352–9362.

(5) (a) Seebach, D.; Abele, S.; Gademann, K.; Juan, B. *Angew. Chem., Int. Ed. Engl.* **1999**, *38*, 1595–1597. (b) For design of a turn structure, see also: Seebach, D.; Abele, S.; Sifferlen, T.; Hänggi, M.; Gruner, S.; Seiler, P. *Helv. Chim. Acta* **1998**, *81*, 2218–2243.

(6) (a) Krauthäuser, S.; Christianson, L. A.; Powell, D. R.; Gellman, S. H. *J. Am. Chem. Soc.* **1997**, *119*, 11719–11720. (b) Chung, Y. J.; Christianson, L. A.; Stanger, H. E.; Powell, D. R.; Gellman, S. H. *J. Am. Chem. Soc.* **1998**, *120*, 10555–10556. (c) Chung, Y. J.; Huck, B. R.; Christianson, L. A.; Stanger, H. E.; Krauthäuser, S.; Powell, D. R.; Gellman, S. H. *J. Am. Chem. Soc.* **2000**, *122*, 3995–4004.

## Scheme 1



of applications for such systems as artificial enzymes (biocatalysts) and perhaps even as therapeutic agents.

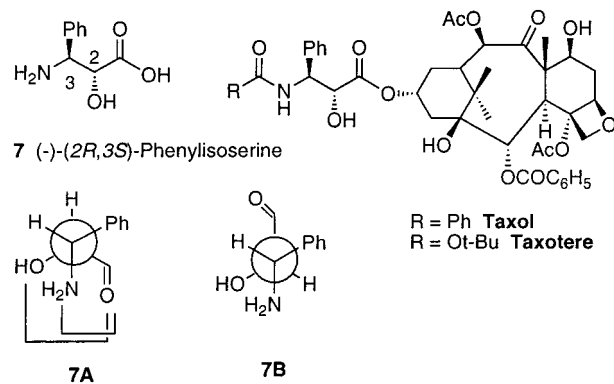
Recognizing that, like natural  $\alpha$ -peptides/proteins, the propensity of the above  $\beta$ -peptide sequences to form stable  $\alpha$ -helix,  $\beta$ -sheet and hairpin structures is determined largely by their ability to form strong geometry-optimized N–H···O=C hydrogen bond networks,<sup>8,9</sup> we defined as an objective the study of  $\beta$ -peptide systems in which additional or alternate opportunities are provided for the formation of secondary structure due to the presence of polar H-bonding donor/acceptor oxygen substituents at the  $\beta^2$  positions on the peptide backbone. In the initial

(7) The factors determining peptide/protein folding are not yet fully elucidated: (a) Duan, Y.; Kollman, P. A. *Science* **1998**, *282*, 740–744. (b) Berendsen, H. J. C. *Science* **1998**, *282*, 642–643. (c) Riddle, D. S.; Santiago, J. V.; Bray, S. T.; Doshi, N.; Grantcharova, V.; Yi, Q.; Baker, D. *Nat. Struct. Biol.* **1997**, *4*, 805–809. (d) Bahar, I.; Atilgan, A. R.; Jernigan, R. L.; Erman, B. *Proteins* **1997**, *29*, 172–185. (e) Fetrow, J. S.; Palumbo, M. J.; Berg, G. *Proteins* **1997**, *27*, 249–271.

(8) Electrostatic (dipole), van der Waals interactions, and side chain entropic effects are also important factors that contribute to the propensity of a given peptide sequence to adopt a helical or other secondary structure. See: (a) Creamer, T. P.; Rose, G. D. *Proc. Natl. Acad. Sci. U.S.A.* **1992**, *89*, 5937–5941. (b) Burley, S. K.; Petsko, G. A. *Adv. Protein Chem.* **1988**, *39*, 125–189. (c) Brandon, C.; Tooze, J. *Introduction to Protein Structure*, 2nd ed.; Garland: New York, **1998**.

(9) (a) Non-hydrogen-bonded helices can be formed from *N*-alkyl glycine and proline oligomers. For a general review, see: Rabanal, R.; Ludevid, M. D.; Pons, M.; Giralt, E. *Biopolymers* **1993**, *33*, 1019. (b) For an example of a  $\beta$ -peptide displaying ordered non-hydrogen-bonded secondary structure, see: Huck, B. R.; Langerhan, J. M.; Gellman, S. H. *Organic Lett.* **1999**, *1*, 1717–1720.

## Scheme 2



evaluation of this concept, a single  $\beta$ -amino acid, phenylisoserine **7**, was chosen as the  $\beta$ -amino acid building unit. This molecule possesses in its structure both a hydrophobic phenyl ring at C-3, and a polar hydroxyl group at C-2. Furthermore, as a direct consequence of research on the taxanes (taxol/taxotere), its natural (–)-(2*R*, 3*S*) and enantiomeric form, as well as the (2*R*, 3*R*) and (2*S*, 3*S*) configurational isomers are readily available by synthesis.<sup>10</sup> Considerable structural diversity can thus be obtained through different combinations of these four phenylisoserine units. This diversity can be further increased by functionalization of the hydroxyl group on the  $\beta^2$  center by groups of differing steric volume and electronic properties. In this latter context, the interaction (repulsive or attractive) of the oxygen substituent with the adjacent hydrophobic phenyl ring and the amide nitrogen can be exploited to bias either gauche or anti conformations and, thereby, modulate and orient movement of the  $\beta$ -peptide chain. The polarity of the solvent medium will be another important factor which will determine the secondary structure that is adopted by phenylisoserine-based  $\beta$ -peptides. The results of both NMR<sup>11</sup> and X-ray<sup>12</sup> diffraction studies show that in apolar solvents such as chloroform, the side chain in taxol/taxotere, and analogues, as well as simple ester/amide derivatives of (–)-(2*R*, 3*S*)-phenylisoserine, adopt a conformation (**7A**) in which the amide nitrogen is gauche to both the C-2 hydroxyl and ester groups. This conformation is stabilized by two five-membered intramolecular hydrogen bond systems [N–H···O (hydroxyl) and O–H···O (carbonyl)]. In contrast, in polar solvents (MeOH and MeOH/water) conformers

(10) (a) In *Enantioselective Synthesis of  $\beta$ -Amino Acids*; Juarisiti, E., Ed.; VCH: Weinheim and New York, **1997**; Chapters 1, 16, and 19–21. (b) Ojima, I.; Delalogue, F. *Chem. Soc. Rev.* **1997**, *26*, 377–386. (c) Jost, S.; Gimbert, Y.; Greene, A. E.; Fotiadu, F. *J. Org. Chem.* **1997**, *62*, 6672–6677. (d) For a general review of  $\beta$ -amino acid synthesis, see: Cole, D. C. *Tetrahedron* **1994**, *50*, 9517–9582.

(11) (a) Miller, R. W.; Powell, R. G.; Smith, C. R., Jr.; Arnold, E.; Clardy, J. *J. Org. Chem.* **1981**, *46*, 1469–1474. (b) Gueritte-Voegelein, F.; Guenard, D.; Mangatal, L.; Potier, P.; Guilhem, J.; Cesario, M.; Pascard, C. *Acta Cryst.* **1990**, *C46*, 781–784. (c) Peterson, J. R.; Do, H. D.; Rogers, R. D. *Pharm. Res.* **1991**, *8*, 908–912. (d) Swindell, C. S.; Krauss, N. E.; Horwitz, S. B.; Ringel, I. *J. Med. Chem.* **1991**, *34*, 1176–1184. (e) Mastro Paolo, D.; Camerman, A.; Luo, Y.; Brayer, G. D.; Camerman, N. *Proc. Natl. Acad. Sci. U.S.A.* **1995**, *92*, 6920–6924. (f) Gao, Q.; Chen, S.-H. *Tetrahedron Lett.* **1996**, *37*, 3425–3428. (g) Gao, Q.; Parker, W. L. *Tetrahedron* **1996**, *52*, 2291–2300.

(12) (a) Dubois, J.; Guénard, D.; Guéritte-Voegelein, F.; Guedira, N.; Potier, P.; Gillet, B.; Beloeil, J.-C. *Tetrahedron* **1993**, *49*, 6533–6544. (b) Vander Velde, D. G.; Georg, G. I.; Grunewald, G. L.; Gunn, C. W.; Mitscher, L. A. *J. Am. Chem. Soc.* **1993**, *115*, 11650–11651. (c) Williams, H. J.; Scott, A. I.; Dieden, R. A. *Tetrahedron* **1993**, *49*, 6545–6560. (d) Paloma, L. G.; Guy, R. K.; Wrasidlo, G. W.; Nicolau, K. C. *Chem. Biol.* **1994**, *1*, 107–112.

(13) For comprehensive theoretical treatment of the taxol side chain conformations, see: Milanese, M.; Ugliengo, P.; Viterbo, D. *J. Med. Chem.* **1999**, *42*, 291–299. (b) See also: Lozynski, M.; Rusinska-Rozsak, R. *Tetrahedron Lett.* **1995**, *36*, 8849–8852.

are preferred (cf. **7B**) in which H<sup>2</sup>/H<sup>3</sup> are anti (hydrophobic collapse).<sup>13–15</sup>

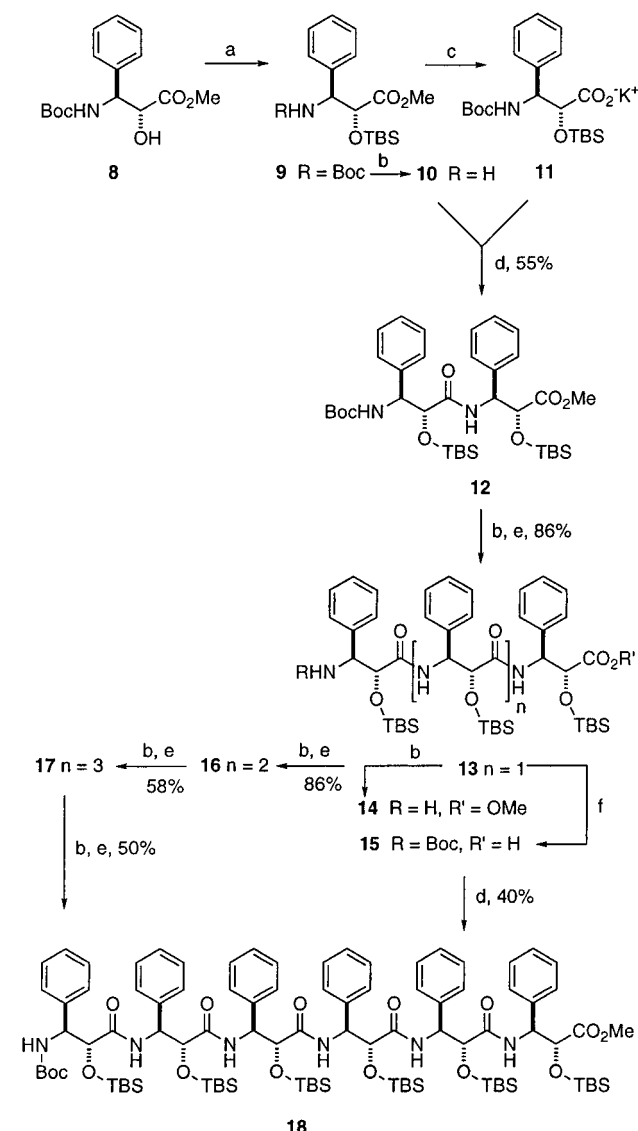
Five- and six-membered H-bonding arrangements are common features in organic chemistry, and are frequently observed in natural products.<sup>16</sup> However, relative to the larger directionally optimized H-bond systems observed in helix and  $\beta$ -sheet structures it is generally considered that five/six-membered H-bonding arrangements contribute little, if at all, to the overall stability of  $\alpha$ -peptides/proteins. Gellman has taken as a premiss that this will also be the case for  $\beta$ -peptide structures.<sup>17,18</sup>

As a first step toward the construction of oligo- $\beta$ -peptides that contain differing variants of the phenylisoserine subunit, the *N*-Boc *O*-*tert*-butyldimethylsilyl-substituted hexa- $\beta$ -peptide ester **18** was constructed from the *O*-TBS ether of (–)-(2*R*, 3*S*)-phenylisoserine (Scheme 2), and its ability to auto-organize in chloroform solution was studied. This particular amino acid was employed because the 2,3-anti (2,3-unlike) stereochemistry of the phenyl and the protected hydroxyl substituents prevent the formation of an  $\alpha$ -helix.<sup>2e</sup> Intrinsic properties of compound **18** brought to light from NMR measurements are its highly preferred and highly stable  $\beta$ -strand-type structure. A repeating series of hydrophobic interactions are observed in this molecule involving the methyl substituents of the *O*-*tert*-butyldimethylsilyl groups. A further repeating motif is the presence of a bifurcated H-bond system involving the amide nitrogen and the carbonyl group of each individual residue and the same NH with the OTBS oxygen atom of the preceding residue *i* – 1.

## Results and Discussion

**Synthesis of Hexa- $\beta$ -peptide 18.** To obtain compound **18**, the free hydroxyl group of *N*-Boc phenylisoserine methyl ester **8**<sup>10</sup> was converted to its *O*-TBDMS ether, affording compound **9** in quantitative yield. Compound **9** was then selectively *N*-deprotected using formic acid in CH<sub>2</sub>Cl<sub>2</sub> to give **10** and *O*-deprotected by treatment with potassium trimethylsilylanolate to give **11**.<sup>19</sup> Coupling of **10** and **11** to give dipeptide **12** (55%) was achieved under Pybop/HOBT conditions using NMM as the base.<sup>20</sup> This compound was in turn *N*-deprotected and coupled with **11** to give tripeptide **13** in 86% yield. Subsequent elaboration of tripeptide **13** to the target molecule **18** was achieved by a convergent route where the free amine derivative **14** and the acid **15**, both derived from **13**, were condensed using Pybop/HOBT. Compound **18** was also obtained in a linear fashion via intermediates **16** and **17** through successive *N*-deprotection and coupling steps with acid **11**. It is noteworthy that the efficiency of coupling decreases from dimer to hexamer (possibly due to hydrophobic repulsion) and that, consequently,

## Scheme 3<sup>a</sup>



<sup>a</sup> (a) TBSCl, Imidazole, DMF, RT, 20 h, 100%. (b) HCO<sub>2</sub>H, CH<sub>2</sub>Cl<sub>2</sub>, RT, 4 h, 100%. (c) KOTMS, Et<sub>2</sub>O, RT, 4 h, 100%. (d) Pybop, NMM, CH<sub>2</sub>Cl<sub>2</sub>, HOBT, RT, 15 h. (e) Conditions (d) plus addition of **11**. (f) KOTMS, Et<sub>2</sub>O, RT, 7 h then reflux 2 h.

the utilization of a large excess of the acid component (up to 6.5 equivs) was necessary to obtain reasonable yields. The former approach proved to be slightly more efficient, providing hexapeptide **18** in 40% overall yield from **13**.  $\beta$ -Peptide **18**, a colorless solid, proved to be completely insoluble in water, and only sparingly soluble in methanol. However, it was highly soluble in chloroform and methylene chloride.

**Circular Dichroism Experiments.** The CD spectra of  $\beta$ -peptides **1–3** with  $\alpha$ -helical structure are strikingly similar to the typical CD pattern of  $\alpha$ -helical proteins (extrema of opposite sign near 200 and 215 nm). Considering that CD absorptions in the region 180–250 nm result mainly from the  $n \rightarrow \pi^*$  (200 nm) and the  $\pi \rightarrow \pi^*$  (190 nm) transitions of the peptide bond,<sup>21</sup> one may thus assume that for  $\beta$ -peptides, the additional C $\beta^3$ –C $\beta^2$  bond will not substantially modify the CD effect.

In the CD spectrum of beta-peptide **18** (CHCl<sub>3</sub>) (Figure 1), a negative Cotton effect with a maximum at 185 nm, and a

(14)  $\beta$ -Peptides designed to be soluble in water, see: (a) Appella, D. H.; Barchi, J. J., Jr.; Durell, S. R.; Gellman, S. H. *J. Am. Chem. Soc.* **1999**, *121*, 2309–2310. (b) Wang, X.; Espinosa, J. F.; Gellman, S. H. *J. Am. Chem. Soc.* **2000**, *122*, 4821–4822. (c) Abele, S.; Guichard, G.; Seebach, D. *Helv. Chim. Acta* **1998**, *81*, 2141–2156.

(15) For a discussion of the influence of solvent on  $\alpha$ -helix formation, see: Kinoshita, M.; Okamoto, Y.; Hirata, F. *J. Am. Chem. Soc.* **2000**, *122*, 2773–2779.

(16) The crystal structure of the macrolide bryostatins serves as an illustrative example: Petit, G. R.; Herald, D. L.; Gao, F.; Sengupta, D.; Herald, C. L. *J. Org. Chem.* **1991**, *56*, 1337–1340.

(17) Dado, G. P.; Gellman, S. H. *J. Am. Chem. Soc.* **1994**, *116*, 1054–1062.

(18) For discussion of five- and six-membered H-bond conformations in  $\beta$ -peptides; see: (a) Gung, B. W.; Zhu, Z. *J. Org. Chem.* **1997**, *62*, 6100–6101. (b) Gung, B. W.; MacKay, J. A.; Zou, D. *J. Org. Chem.* **1999**, *64*, 700–706. (c) See also refs 4e and 4f.

(19) Laganis, E. D.; Chenard, B. L. *Tetrahedron Lett.* **1984**, *25*, 5831–5834.

(20) Coste, J.; Le-Nguyen, D.; Castro, B. *Tetrahedron Lett.* **1990**, *31*, 205–208.

(21) Cantor, C. R.; Schimmel, P. R. *Biophysical Chemistry, Part II, Techniques for the Study of Biological Structure and Function*, W. H. Freeman and Company: New York, 1980.

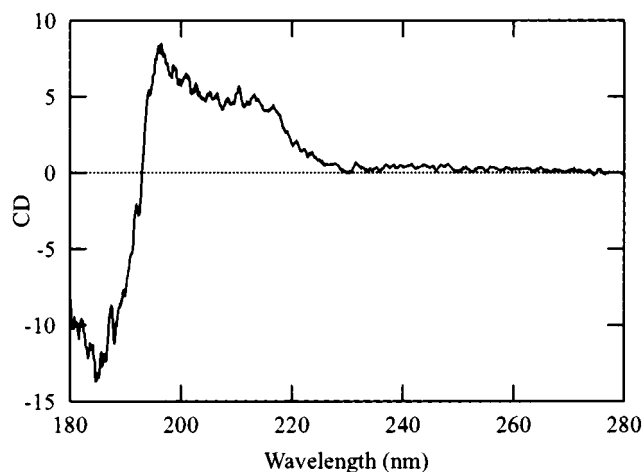


**Figure 1.** CD spectrum of homo- $\beta$ -peptide **18** (0.1 nM in  $\text{CDCl}_3$ , 1-mm path length).

positive effect of lower amplitude in the region 196–220 nm was observed. This latter broad absorption is composed of two maxima, centered respectively at 200 and 210 nm. These extrema of opposite signs indicate that the molecule possesses a defined nonhelical secondary structure (absence of the typical negative minimum at 215–220 nm).

By analogy to the spectra for polypeptides derived from  $\alpha$ -amino acids, the optical behavior of  $\beta$ -peptide **18** resembles more closely that for an elongated conformation, such as a twisted  $\beta$ -strand, a  $\beta$ -turn, or even a distorted  $\alpha$ -helix. On this assumption, and given the dependence of the CD spectral pattern on geometrical factors,<sup>22</sup> the presence of two positive maxima at 200 and 210 nm suggests that two distinct phenomena are in play. This may correspond to either two different peptide conformer populations or to a single population plus a contribution from another source such as the phenyl rings. In fact, the interpretation of the CD spectrum of  $\beta$ -peptide **18** is complicated by the presence of the six phenyl groups,<sup>23</sup> making it difficult to predict the molecule's secondary structure from the CD data alone.

**NMR-Determined Structure.** In the  $^1\text{H}$  NMR spectrum of **18** (500 MHz), it was remarkable to observe that even though the molecule is composed of six identical repeating units, distinct resonances were observed for the NH (6.0–8.5 ppm) and the six  $\text{C}\beta^2\text{-H}$  protons (3–4.5 ppm) (Figure 2). No significant differences were observed between the spectra that were obtained for differing concentrations of **18**, which indicates that the molecule exhibits no tendency toward aggregation. In addition, well-defined cross-peaks were observed for each  $\beta$ -amino acid residue in the DQF-COSY and TOCSY spectra, which permitted the identification of the individual NH,  $\text{C}\beta^3\text{-H}$ , and  $\text{C}\beta^2\text{-H}$  resonances.

From subsequent analysis of the long distance  $\text{C}_i\text{H}\beta^2i$  and  $\text{C}_i\text{NH}i + 1$  couplings in the HMBC spectrum it was possible to make peak assignments for the entire molecular backbone of hexa- $\beta$ -peptide **18**. In particular, the chemical shift characteristic for the Boc C=O group enabled the identification of the amide proton in the first residue (module), and the absence of the correlation  $\text{C}_i\text{NH}i + 1$  permitted the location of the amide carbonyl absorption in the C-terminal residue (module 6).

Assignment of the phenyl ring and the (*tert*-butyl)dimethylsilyl group in each module was possible by using the spatial

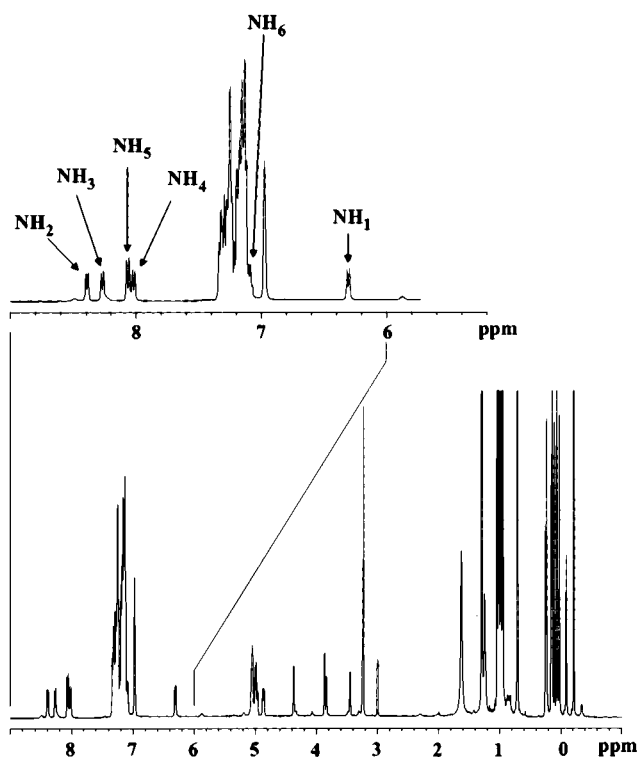


**Figure 2.** One-dimensional  $^1\text{H}$  NMR spectrum of homo- $\beta$ -peptide **18** in  $\text{CDCl}_3$  at 298 K.

**Table 1.**  $^1\text{H}$  NMR Chemical Shifts in ppm for Homo- $\beta$ -peptide **18**

module	NH	$\beta^3\text{H}$	$\beta^2\text{H}$	<i>t</i> -butyl	Si-CH <sub>3</sub>	phenyl	module
1	6.3	5.04	4.37	0.98	0.066	-0.087	7.22/7.26
2	8.39	5.05	3.84	1.018	0.25	0.157	7.3
3	8.27	5.06	3.45	1.042	0.235	0.139	7.24
4	8.02	4.97	3.25	0.95	0.105	0.025	7.16
5	8.06	4.87	3	0.95	0.139	0.066	7.13
6	7.18	5	3.87	0.709	-0.212	-0.212	7.13

Boc: 1.3 ppm. OMe: 3.23 ppm.

**Table 2.** Coupling Constants in Hz for Homo- $\beta$ -peptide **18**

module	$J(\text{NH},\beta^2\text{H})$	$J(\beta^3\text{H},\beta^2\text{H})$
1	9.2	2.9
2	9.6	3.9
3	9.6	3.7
4	10	3.4
5	11	3.9
6	n.d.	2.3

internal correlations that were observed in the ROESY spectra, because strong cross-peaks were observed between  $\text{C}\beta^3\text{-H}$  and the phenyl-ring protons and between  $\text{C}\beta^2\text{-H}$  and the signals for both the *tert*-butyl group and the methyls that were attached directly to silicon. It is noteworthy that, with the exception of module 6, the two SiMe groups in the five remaining O-TBS systems have distinct chemical shifts. This is consistent with hindered rotation about the  $\text{C}\beta^2\text{-O-Si}$  bonds.

The complete set of  $^1\text{H}$  chemical shift values and coupling constants for **18** are presented in Tables 1 and 2. From the data, and in particular from the finding that there is a chemical shift dispersion for the same entities between modules and that the coupling constants are not averaged out, it becomes apparent that homo- $\beta$ -peptide **18** adopts a stable ordered secondary structure in chloroform solution. This conclusion was reinforced by the results of amide proton exchange studies which showed that, whereas NH-1 and NH-6 exchange rapidly, no proton

(22) Manning, M. C.; Illangasekare, M.; Woody, R. W. *Biophys. Chem.* **1988**, *31*, 77–86.

(23) Manning, M. C.; Woody, R. W. *Biochemistry* **1989**, *28*, 8609–8613.

exchange for NH-2 to NH-5 was detected after 4 days in CD<sub>3</sub>-OD (see Supporting Information). This observation, together with the downfield chemical shifts of NH-2 through NH-5 (ranging from 8.06 to 8.39 ppm) provided a first indication that these amide protons are involved in hydrogen bonds.

Having assigned all of the proton signals, the following step was to achieve a quantitative interpretation of the spectra in terms of both the dihedral angle constraints derived from the  $J(\text{NH}, \text{H}-\text{C}\beta^3)$  and  $J(\text{H}-\text{C}\beta^3, \text{H}-\text{C}\beta^2)$  couplings calculated from the 1D spectra, and the distance constraints estimated from all of the cross-peaks in the ROESY spectra. By recording the spectra at different mixing times, it was determined that the intensities were not influenced by spin diffusion (strong/medium intensity ratio remained constant). Thus, NOE assignment was made from the spectra with the least baseline noise (mixing time, 200 ms). Furthermore, with the exception of an exchange cross-peak detected for NH-1 (flexible N-terminal region) the correlation pattern depicted in the ROESY spectra was consistent with a unique folding of the molecule.

Unlike the spectra for  $\beta$ -peptide **3**,<sup>2a</sup> no NOE peaks were detected between the NH<sub>*i*</sub> and the C $\beta^3$ -H of residues  $i + 2$  or  $i + 3$ . Indeed, for the peptide backbone, only correlation peaks internal to each module or between two consecutive modules were observed. It is also important that, contrary to what is found for  $\alpha$ -helix structures, only one NH/NH NOE between modules 1 and 2 was observed. However, as is characteristic for a  $\beta$ -strand structure in natural peptides, six internal NH-H $\beta^2$  NOE signals, all identical and intense, and five sequential H $\beta^2(i - 1)$ -NH NOEs were detected, also identical, albeit weaker in intensity. The data were, thus, inconsistent with a helix folding pattern, but were consistent with an elongated conformation for the molecule.

The calculation of the three-dimensional structure of **18** from the NMR data proved not to be straightforward. This was due to the absence of a suitable reference distance that would permit interpretation of the NOE intensities in terms of interproton distance constraints. Indeed, because the structures of oligomers of phenylisoserine have not previously been studied, no structural criterion could be used to interpret any of the peak heights. Furthermore, due to proton resonance overlap for the methyl groups and those for the *ortho* and *para* protons within each phenyl ring, an unequivocal measurement of the NOE peak intensities for intra-spin system cross-peaks within each entity was not possible. To circumvent this situation, distance constraints were introduced and refined through an iterative process during the calculations, which verified at each step the correspondence between the geometrical characteristics of the generated structures and the experimental data.

Precise information concerning the backbone torsion angles could be extracted from the coupling constants  $J(\text{NH}, \text{H}-\text{C}\beta^3)$  and  $J(\text{H}-\text{C}\beta^3, \text{H}-\text{C}\beta^2)$  using Karplus equations. However, this translation gave rise to a series of different spatial organizations. The five couplings  $J(\text{NH}, \text{H}-\text{C}\beta^3)$ , all larger than 9 Hz, led to two angular intervals, both of which are consistent with a trans conformation, that is,  $[150^\circ, 180^\circ]$  and  $[-180^\circ, -150^\circ]$ . The six couplings  $J(\text{H}-\text{C}\beta^3, \text{H}-\text{C}\beta^2)$ , ranging from 2 to 4 Hz, imposed two cis angular orientations of the C $\beta^3$ -C $\beta^2$  bond, that is,  $[60^\circ, 120^\circ]$  and  $[-120^\circ, -60^\circ]$ . Four angular situations were ultimately taken into account during the first calculation in order to explore a priori all the allowed conformational space.

After having introduced the theoretical constraints corresponding to the 2*R*,3*S* configuration of the  $\beta^2$ - and  $\beta^3$ -carbons centers, as well as the angle constraints inherent to the peptide bond ( $\text{O}-\text{C}-\text{N}-\text{H} = 160-180^\circ$ ), a preliminary series of

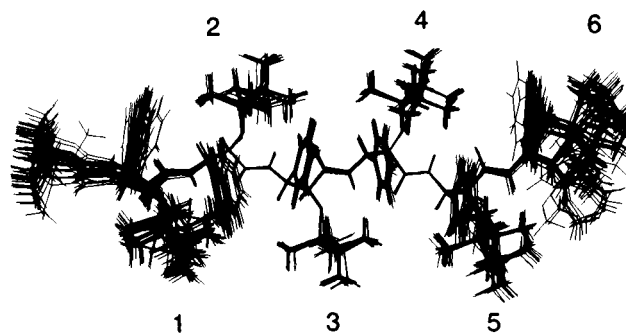


**Figure 3.** Overlay of the 24 best structures of homo- $\beta$ -peptide **18** as determined by NMR spectroscopy and constrained molecular dynamics simulations.

**Table 3.** Mean Torsion Angles of Homo- $\beta$ -peptide **18**

$(\text{O}=\text{C})-\text{N}-\text{C}\beta^3-\text{C}\beta^2$	$-147.0 \pm 6.0^\circ$
$\text{N}-\text{C}\beta^3-\text{C}\beta^2-\text{C}(=\text{O})$	$-66.0 \pm 2.0^\circ$
$\text{C}\beta^3-\text{C}\beta^2-\text{C}(=\text{O})-\text{N}$	$-132.0 \pm 5.0^\circ$
$\text{N}-\text{C}\beta^3-\text{C}\beta^2-\text{O}$	$168.0 \pm 2.0^\circ$
$\text{O}-\text{C}\beta^2-\text{C}=\text{O}$	$173.0 \pm 5.0^\circ$
$\text{H}-\text{N}-\text{C}\beta^3-\text{C}(\text{Ph})$	$-92.0 \pm 8.0^\circ$
$\text{C}\beta^3-\text{C}\beta^2-\text{O}-\text{Si}$	$-97.0 \pm 3.0^\circ$
$\text{C}\beta^2-\text{O}-\text{Si}-\text{C}(\text{H}_3)_3$	$-80^\circ/179^\circ$

structures were generated using only unambiguous experimental data. In this way, NOEs of strong intensity observed between each internal NH-C $\beta^2$ H, and NOEs of medium intensity between consecutive modules C $\beta^2$ H( $i - 1$ )-NH<sub>*i*</sub> could be translated into distance intervals  $[2.0 \text{ \AA}, 3.0 \text{ \AA}]$  and  $[3.0 \text{ \AA}, 5.0 \text{ \AA}]$ , respectively. To avoid prohibited conformational sampling, the lack of a NOE cross-peak between two protons was also considered by introducing a lower distance boundary of 5  $\text{\AA}$ . The lower limit for the internal distances NH-*t*-Bu and the consecutive distances NH-NH, H $\beta^2$ -H $\beta^2$  and phenylisoserine, PhH-NH, was thus imposed. Note, however, that all NOEs involving methyl groups or aromatic protons were not retained during this preliminary step because the peak intensities could not be transformed into distances as a consequence of proton chemical shift degeneracy.

A total of 50 structures were generated with a first series of constraints. The confrontation of the geometrical characteristics of this set of structures with the experimental data immediately permitted a better definition of the constraints. The dihedral angles H-N-C $\beta^3$ -H and H-C $\beta^3$ -C $\beta^2$ -H were, thus, restrained to the intervals  $[150^\circ, 160^\circ]$  and  $[-60^\circ, -50^\circ]$ , respectively. The list of constraints was completed by introduction of distance intervals relative to spatial proximities that were detected on the ROESY spectra between the H $\beta^2$  proton and the phenyl ring and between H $\beta^3$  and the closest Si(CH<sub>3</sub>) within each module. Distance restraints relative to the weak NOEs observed between the degenerate methyls of the *tert*-butyl group of module  $i$  and the  $\beta^2$  proton of module  $i + 2$  were also included. Finally, a total of 12 chirality constraints, 17 angle restraints, and 100 distance restraints were used for the computation of a new batch of structures (see Supporting Information). Several cycles of calculation were run to improve, where necessary, the definition of the constraint intervals until the conformers with the lowest violation and the lowest energy were obtained.

From this calculation, 24 structures were selected. All of them converged to the same fold, with no violations larger than 0.4  $\text{\AA}$  or 2.5°. These structures are shown superimposed onto the best-fitted structure in Figure 3. The root-mean-square deviation (rmsd) is 0.24 and 1.56  $\text{\AA}$  for the N, C $\beta^3$ , C $\beta^2$ , C=O backbone atoms, and all heavy atoms, respectively. The structure is, thus,

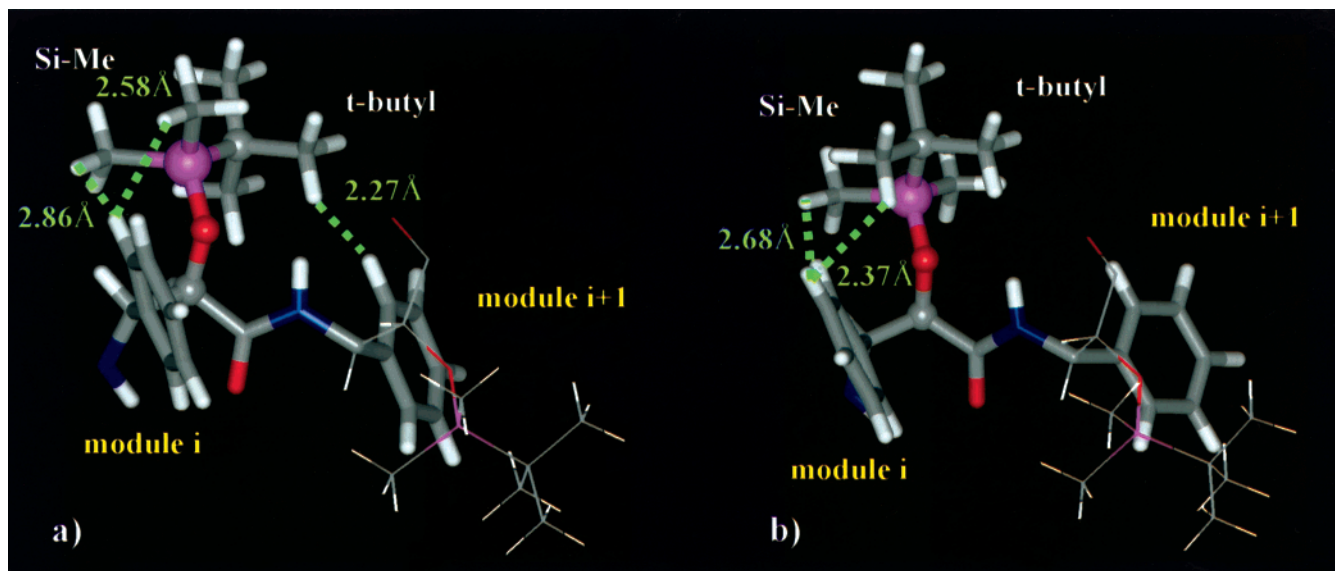


Figure 4. a, b: OTBS–phenyl group interactions.

better described for the backbone than for the side-chain conformation. The backbone of modules 2–5 appears particularly well-overlaid, with a rmsd of 0.11 Å, which suggests a greater rigidity for this peptide segment. The most important conformational changes occur at both termini of the  $\beta$ -peptide, which is consistent with a greater flexibility of this region of the molecule (evidenced by the rapid NH–ND exchange rate observed for module 1 and 6).

As seen, the main chain of the  $\beta$ -peptide **18** adopts an extended  $\beta$ -strand-type conformation in  $\text{CHCl}_3$  solution, whose mean backbone dihedral angles are indicated in Table 3. Immediately apparent from the data is that each of the six modules adopts essentially the same conformation in which the  $\text{N}-\text{C}\beta^3-\text{C}\beta^2-\text{C}(=\text{O})$  torsion angle is  $-66^\circ$ . Thus, within each module, a gauche relationship exists between the NH and the amide  $\text{C}=\text{O}$  as well as between the phenyl and the *O*-TBS-protected oxygen substituent. In this conformation, the NH and OTBS groups are almost peri-antiplanar ( $168^\circ$ ), and the  $\text{C}\beta^2-\text{O}$  bond is pointing in the opposite direction to the amide carbonyl ( $\text{O}=\text{C}-\text{C}\beta^2-\text{O} = 173^\circ$ ).

Further consequences of the gauche  $\text{N}-\text{C}\beta^3-\text{C}\beta^2-\text{C}(=\text{O})$  torsion angle are that the amide carbonyls of adjacent residues are oriented in opposing directions and that with respect to module  $i$  ( $g^+$ ), the module  $i+1$  is “upside down” ( $g^-$ ).<sup>6a</sup> Thus, on going from module 1 to module 2, the phenyl ring changes sides (rotation of  $150^\circ$ ). Continuing to module 3, it returns to the same side of the molecule as for module 1, but it is shifted in an anticlockwise sense by approximately  $-60^\circ$ . From this observation, one can deduce that longer  $\beta$ -peptide oligomers of *O*-TBS-protected (2*R*, 3*S*)-phenylisoserine would form a very elongated twist, with one complete turn every 13 residues.

By looking more closely at the phenyl ring orientation, one sees that the  $\text{H}-\text{N}-\text{C}\beta^3-\text{C}(\text{Ph})$  dihedral angle is  $-92^\circ$ . The adjacent NH bond is, thus, almost perpendicular to the  $\text{C}\beta^3-\text{C}(\text{Ph})$  bond and, indeed, to the plane of the ring. The NH is, thus, positioned in the negative anisotropic zone of the aromatic ring, and this, together with the involvement of the amide hydrogen in hydrogen bonding (vide infra), would account for the particularly marked downfield chemical shift of four of the six amide protons. From a measure of the dihedral angles, it was further found that the angle between two adjacent phenyl rings is  $\pm 178^\circ$ , which indicates that they are essentially parallel, and between phenyl rings in modules  $i$  and  $i+2$ , an angle of

$-30^\circ$  is observed. The mean distance between these phenyl rings is approximately 9 Å.

The dihedral angle  $\text{C}\beta^3-\text{C}\beta^2-\text{O}-\text{Si} = -97^\circ$  is relatively fixed, which indicates that there is hindered rotation about the  $\text{C}\beta^3-\text{O}$  bond. The  $\text{O}-\text{Si}$  bond is, thus, more or less perpendicular to the  $\text{C}\beta^3-\text{C}\beta^2$  bond and points away from the phenyl ring. The orientations of the two methyls and the freely rotating *tert*-butyl group around the silicon atom are described by the dihedral angles  $\text{C}\beta^2-\text{O}-\text{Si}-\text{C}(\text{CH}_3)_3 = -80^\circ$  and  $\pm 179^\circ$ . From the mean values derived from analysis of the 24 NMR structures, it is clear that the OTBS side-chain orientations in modules 2 and 3 ( $-80^\circ$ ) are better determined and, thus, relatively immobile when compared to the other residues.

In the solution structure of  $\beta$ -peptide **18**, there is a high degree of similitude between modules. This gives rise to a series of interactions which are repeated along the peptide chain. These cumulative interactions are at the origin of the remarkable conformational stability of the molecule.<sup>24</sup>

Consider first the van der Waals-type interactions of the *tert*-butyldimethylsilyl groups on oxygen with their surrounding environment. As depicted in Figure 4a, when the  $\text{C}\beta^2-\text{O}-\text{Si}-\text{C}(\text{CH}_3)_3$  dihedral angle is  $-80^\circ$ , the  $\text{Si}-\text{C}(\text{CH}_3)_3$  bond is approximately perpendicular to the  $\text{C}\beta^2-\text{O}$  bond. In this orientation the two Si-methyl groups point toward the phenyl ring of the same module [ $\text{Si}-\text{CH}_3-\text{A}$  distance/angle: ( $\text{Si}-\text{CH}_3$ )H–H(Ph) = 2.58 Å,  $\text{C}(\text{Ph})-\text{H}(\text{Ph})\cdots\text{H}(\text{SiCH}_3) = 131^\circ$ ] [ $\text{Si}-\text{CH}_3-\text{B}$  distance/angle: ( $\text{Si}-\text{CH}_3$ )H–H(Ph) = 2.86 Å,  $\text{C}(\text{Ph})-\text{H}(\text{Ph})\cdots\text{H}(\text{SiCH}_3) = 143^\circ$ ], whereas the three degenerate methyls of the *tert*-butyl group are oriented toward the phenyl ring of the next module [*tert*-butyl  $\text{CH}_3$  distance/angle: (*t*-Bu)H–H(Ph) = 2.27 Å,  $\text{C}(\text{Ph})-\text{H}(\text{Ph})\cdots\text{H}(\text{t-Bu}) = 155^\circ$ ].

Alternatively, when  $\text{C}\beta^2-\text{O}-\text{Si}-\text{C}(\text{CH}_3)_3 = \pm 180^\circ$ , the  $\text{Si}-\text{C}(\text{CH}_3)_3$  bond is collinear to the  $\text{C}\beta^2-\text{O}$  bond (Figure 4b). In this instance, one of the silyl methyls and one the *tert*-butyl methyls points toward the phenyl ring of the same module [ $\text{Si}-\text{CH}_3$  distance/angle: ( $\text{Si}-\text{CH}_3$ )H–H(Ph) = 2.68 Å,  $\text{C}(\text{Ph})-\text{H}(\text{Ph})\cdots\text{H}(\text{SiCH}_3) = 150^\circ$ ] [*tert*-butyl  $\text{CH}_3$  distance/angle: (*tert*-Bu)H–H(Ph) = 2.37 Å,  $\text{C}(\text{Ph})-\text{H}(\text{Ph})\cdots\text{H}(\text{t-Bu}) = 100^\circ$ ].

To explore in more detail the orientation of the OTBS group

(24) Other  $\beta$ -peptide systems displaying ordered  $\beta$ -strand-type backbone structures. Oligoanthranilimides: (c) Hamuro, Y.; Geib, S. J.; Hamilton, A. D. *J. Am. Chem. Soc.* **1997**, *119*, 10587–10593.  $\beta$ -hexa-alanyl PNA: Diederichsen, U.; Schmitt, H. W. *Eur. J. Org. Chem.* **1998**, *827*, 7–835.

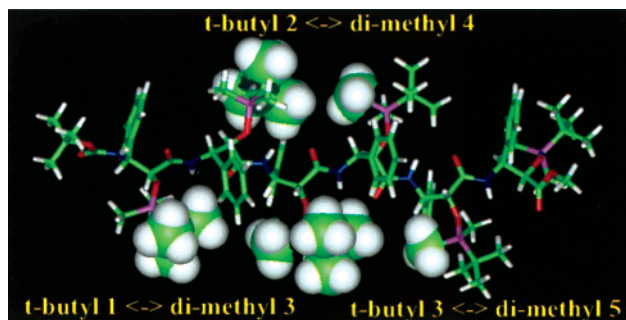


**Figure 5.** van der Waals-type interactions between the Si-*tert*-butyl methyl groups on residue *i* and the Si-Me groups on residue *i* + 2.

in **18**, the  $C\beta^2-O-Si-C(CH_3)_3$  dihedral angle was modified using INSIGHT tools (Molecular Simulations Inc.). It was found that different positions may be occupied without steric conflict. However, only the angular positions  $-80^\circ, \pm 179^\circ$  resulted in the short Si(CH<sub>3</sub>)<sub>i</sub>/phenyl ring, C(CH<sub>3</sub>)<sub>3</sub>/phenyl ring *i* + 1, C(CH<sub>3</sub>)<sub>3</sub>/phenyl ring *i* distances that are systematically observed. The orientation of the OTBS group relative to the phenyl ring, thus, appears to represent the best compromise between hydrophobic (CH- $\pi$ -type) interactions and steric hindrance that can be achieved for the *gauche* conformation of these substituents.

These interactions are reflected in the chemical shift displacements (Table 1). Indeed, in modules 2 and 3 where the dihedral angle is  $-80^\circ$ , the *tert*-butyl methyl proton signal is at lower field, and inversely, the Si-Me proton signals are at a higher field than for modules 1, 4, and 5. In these latter modules, the chemical shift values represent a statistical distribution of the orientations  $-80^\circ$  and  $\pm 179^\circ$ .

For module 6, with the highest degree of flexibility, both the Si-methyl and the *tert*-butyl proton absorptions are shifted upfield, which suggests that these groups are oriented face-on with respect to the phenyl ring, that is, they also experience a CH- $\pi$  interaction.

A further, and very important, property of the positioning of the OTBS groups is the creation of a network of van der Waals contacts involving a *tert*-butyl methyl group on residue *i* with one of the Si-methyl groups on residue *i* + 2, observed between residues 1 and 3, 3 and 5, and 2 and 4 (distance H-H: 3.4 Å, as expected from the NOE data) (Figure 5). Although such hydrophobic interactions are individually weak, they most probably contribute in an additive fashion to hold the molecule in the observed conformation.

A second important role played by the OTBS group on the  $\beta^2$ -center in **18** is the involvement of the oxygen atom in a network of intramolecular hydrogen bonds. Illustrated in Figures 6 and 7 is the fact that the O-Si(CH<sub>3</sub>) in module *i*, and the NH and C=O groups in module *i* + 1 are basically located in the same plane, with short distances between the NH hydrogen and the flanking carbonyl oxygen and OTBS oxygen atoms. This architecture is translated in terms of an inter-(five-membered)/intra-(six-membered) module bifurcated H-bonding system [five-membered: O<sub>i</sub>⋯NH<sub>*i*+1</sub>, mean distance O⋯HN = 2.26 Å, mean angle formed by O⋯H-N = 109°; six-membered: NH<sub>*i*</sub>⋯(O=C)<sub>*i*+1</sub>, mean distance NH⋯O = 2.35 Å, mean angle formed by N-H⋯O=C = 118°], which spans the length of the peptide, thus consolidating its  $\beta$ -strand structure.

It has been argued that intraresidue hydrogen bonding, and H-bonding between adjacent residues will contribute little to the secondary structure of  $\beta$ -peptides<sup>17</sup> because, for geometrical reasons, such H-bonds are necessarily weaker than alternate possibilities which lead to  $\alpha$ -helices,  $\beta$ -sheets, and  $\beta$ -turns.

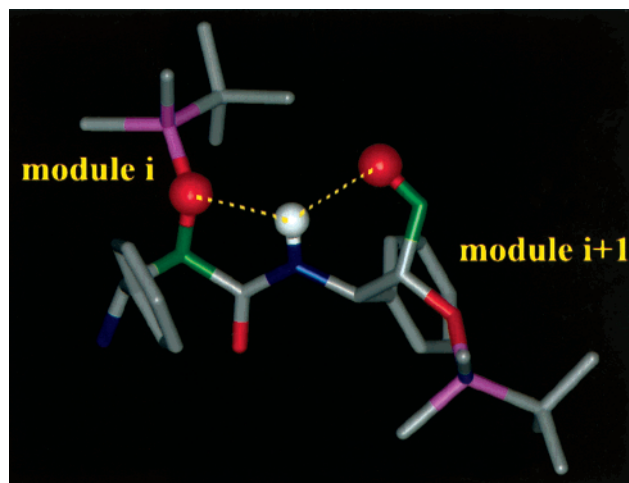
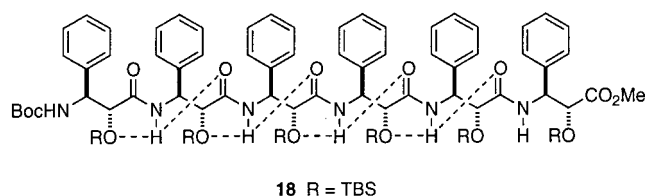


**Figure 6.** Inter(five-membered)/Intra(six-membered) bifurcated hydrogen bond network.



**18** R = TBS

**Figure 7.** Graphic representation of the inter(five-membered)/intra(six-membered) bifurcated hydrogen bond network in homo- $\beta$ -peptide **18**.

However, such arrangements have been documented for specific  $\alpha$ -peptide fragment,<sup>25</sup> and are a fundamental feature in certain  $\beta$ -peptide oligomers.<sup>24</sup> Theoretical studies of  $\beta$ -peptide folding also suggest the existence of six-membered H-bonding conformations.<sup>4e,f</sup>

As mentioned earlier, intramolecular H-bonding has been observed and evoked as an important feature in the conformation adopted in CHCl<sub>3</sub> by the side chain of taxol/taxotere.<sup>11,12</sup> Indeed, this property of phenylisoserine **7** is one of the reasons why this entity was chosen as the monomer unit in the construction of the homo- $\beta$ -peptide **18**. In a theoretical model developed by Viterbo et al.,<sup>13a</sup> it was suggested that only the O-H⋯O (carbonyl) interaction contributes significantly to the stability of **7**, while the N-H⋯O (hydroxyl) interaction is purely electrostatic (dipole-dipole) in nature. Furthermore, it is suggested that the former interaction is due more to the shielding of the O (hydroxyl)⋯O (carbonyl) Coulombic repulsion by the interposed hydrogen than to the formation of a hydrogen bond. At present, no quantitative evaluation of the stabilizing effect of the hydrogen bonding network detected in structure **18** is available; however, these H-bonds are clearly weak because neither the distances nor the angles are optimal.<sup>8b,26</sup> This constatation leads us to suspect that the van der Waals interactions involving the OTBS methyl groups and H-bonding operate in concert to privilege the highly solution-stable secondary structure adopted by **18**. Indeed, it may well be that the one of these through-space interactions alone would be insufficient to stabilize the  $\beta$ -strand conformation.

(25) (a) Crisma, M.; Formaggio, F.; Toniolo, C.; Yoshikawa, T.; Wakamiya, T. *J. Am. Chem. Soc.* **1999**, *121*, 3272-3278. (b) Toniolo, C. *CRC Crit. Rev. Biochem.* **1980**, *9*, 1-44.

(26) A quantitative description of H-bonds has recently been achieved. See ref 1 in: Martin, T. W.; Derewenda, Z. S. *Nature Struct. Biol.* **1999**, *6*, 403-406.

## Conclusion

From this study, it is seen that the oxygen substituent at  $C\beta^2$  in the  $\beta$ -peptide monomer unit plays a determining role in stabilizing the secondary structure of  $\beta$ -peptide **18**. In light of this finding, it is interesting to speculate what will occur if, for instance, two strands of this molecule are connected to a  $\beta$ -turn element to give a structure analogous to **6**.<sup>6a</sup> Note that both the N- and C-terminal fragments in **6** and the phenylisoserine units in **18** possess the  $\beta^2, \beta^3$ -unlike configuration. However, whereas a  $N-C\beta^3-C\beta^2-C(=O)$  gauche conformation is preferred for **18**, the corresponding fragments in **6** adopt the anti conformation, in part so as to minimize unfavorable steric interactions between the bulky  $\beta^2$  and  $\beta^3$  substituents. The important question one can ask concerning a peptide containing two **18** subunits joined by a hairpin motif is whether the conformation of each **18** component held together by the weak but combined van der Waals/hydrogen bond interactions will be disrupted in favor of formation of an anti-conformation  $\beta$ -sheet structure which is stabilized by strong interstrand hydrogen bonds. The study of such a structure, both in chloroform and more polar solvents, will thus provide valuable information concerning the magnitude of the forces that stabilize the conformation of **18**.

Finally, a pertinent point concerning the secondary structural features of phenylisoserine based  $\beta$ -peptides is the consequence of changing the configuration at the  $\beta^3$  center. Seebach has shown that  $\beta$ -peptides with the  $\beta^2, \beta^3$ -like configuration can fold to give helix structures because the two substituents will occupy lateral positions.<sup>2c</sup> However, a molecular model of the homohexapeptide constructed from (2*S*,3*S*)-phenylisoserine suggests an alternative extended  $\beta$ -strand structure in which van der Waals interactions involving the OTBS groups in residues  $i$  and  $i + 1$  again play a major role. The crucial feature of this model structure relative to **18** is the positioning of the phenyl group directly in between the two TBS groups such that the hydrophobic interaction is of the CH- $\pi$ -type, that is, the silyl methyl and *tert*-butyl methyl groups interact  $\ll$  through  $\gg$  the  $\pi$ -system of the aromatic ring. Further work is currently being pursued to validate this prediction.

## Experimental Section

***N*-tert-Butoxycarbonyl-*O*-tert-butylidimethylsilylphenylisoserine Methyl Ester (9).** To a solution of *N*-tert-butoxycarbonylphenylisoserine methyl ester **8** (2.00 g, 6.77 mmol) in dry DMF (5 mL) was added *tert*-butyldimethylsilyl chloride (4.59 g, 30.48 mmol, 4.5 equivs) and imidazole (4.15 g, 60.96 mmol, 9 equivs). The resultant mixture was stirred for 20 h at room temperature under nitrogen then diluted with  $CH_2Cl_2$  (150 mL) and washed with brine. The aqueous washings were extracted with  $CH_2Cl_2$  (3  $\times$  100 mL), and the organic layers were combined, dried over  $Na_2SO_4$ , and concentrated under vacuum. The oily residue was purified by flash column chromatography on silica gel (heptane, then heptane-EtOAc, 2:1), affording after prolonged drying under vacuum<sup>27</sup> *N*-tert-butoxycarbonyl-*O*-tert-butylidimethylsilylphenylisoserine methyl ester **9** as a colorless oil (2.80 g; 100%);  $R_F$  0.76 (1:1, heptane:EtOAc);  $^1H$  NMR (250 MHz,  $CDCl_3$ )  $\delta$  -0.36 (s, 3H), -0.18 (s, 3H), 0.74 (s, 9H), 1.42 (s, 9H), 3.76 (s, 3H), 4.38 (s, 1H), 5.20 (d,  $J = 9.1$  Hz, 1H), 5.52 (d,  $J = 9.1$  Hz, 1H), 7.21-7.35 (m, 5H);  $^{13}C$  NMR (62.89 MHz,  $CDCl_3$ )  $\delta$  -5.94, -5.53, 18.28, 25.59, 28.39, 52.26, 57.25, 75.93, 79.80, 126.62, 127.48, 128.38, 139.78, 155.27, 171.85;  $[\alpha]_D^{20} + 7.4^\circ$  ( $c = 2.16$ ,  $CH_2Cl_2$ ); Anal. Calcd for  $C_{21}H_{35}NO_5Si$ : C, 61.58; H, 8.62; N, 3.42. Found: C, 61.71; H, 8.81; N, 3.41.

***O*-tert-Butyldimethylsilylphenylisoserine Methyl Ester (Formate Salt) (10).** A solution of *N*-tert-butoxycarbonyl-*O*-tert-butylidimethyl-

silylphenylisoserine methyl ester **9** (0.89 g, 2.2 mmol) in a 1:1 v:v mixture of  $CH_2Cl_2$  and formic acid (20 mL) was stirred for 4 h at room temperature under nitrogen. The solvent was then evaporated, and the residue was dried under vacuum until a solid was obtained. The resulting solid was washed with a small amount of ether and dried under vacuum giving *O*-tert-butylidimethylsilylphenylisoserine methyl ester-HCO<sub>2</sub>H **10** as a white solid (0.77 g; 100%);  $^1H$  NMR (200 MHz,  $CDCl_3$ )  $\delta$  -0.15 (s, 3H), -0.07 (s, 3H), 0.82 (s, 9H), 3.67 (s, 3H), 4.47 (d,  $J = 4.0$  Hz, 1H), 4.63 (d,  $J = 4.0$  Hz, 1H), 7.36 (m, 5H), 8.10 (br.s, 2H).

**Potassium *N*-tert-butoxycarbonyl-*O*-tert-butylidimethylsilylphenylisoserinate (11).** To a solution of *N*-tert-butoxycarbonyl-*O*-tert-butylidimethylsilylphenylisoserine methyl ester **9** (0.90 g, 2.2 mmol) in dry ether (50 mL) was added potassium trimethylsilanolate (0.31 g, 2.42 mmol, 1.1 equivs), and the mixture was stirred for 4 h at room temperature under nitrogen. After the first 15-20 min, the formation of a voluminous white precipitate was observed. The solvent was then evaporated, and the solid residue was washed with heptane-ether (1:1). Drying in a vacuum afforded potassium *N*-tert-butoxycarbonyl-*O*-tert-butylidimethylsilylphenylisoserinate **11** as a white solid (0.96 g; 100%);  $^1H$  NMR (200 MHz,  $CDCl_3$ )  $\delta$  0.00 (s, 3H), 0.10 (s, 3H), 0.94 (s, 9H), 1.55 (s, 9H), 4.35 (d,  $J = 2.8$  Hz, 1H), 5.25 (br s, 1H), 6.43 (br s, 1H), 7.37-7.48 (m, 5H).

**Boc-Dipeptide-OMe (12).** To a solution of potassium *N*-tert-butoxycarbonyl-*O*-tert-butylidimethylsilylphenylisoserinate **11** (1.38 g, 3.18 mmol, 1.3 equivs) in dry  $CH_2Cl_2$  (30 mL) at 0  $^\circ C$  under nitrogen was added Pybop (1.82 g, 3.50 mmol, 1.4 equivs), followed by a solution of *O*-tert-butylidimethylsilylphenylisoserine methyl ester-HCO<sub>2</sub>H **10** (0.87 g, 2.44 mmol) in  $CH_2Cl_2$  (10 mL), and *N*-methylmorpholine (NMM) (0.77 mL, 7.00 mmol, 2.8 equivs). The mixture was stirred for 5 min at 0  $^\circ C$  before adding hydroxybenzotriazole (0.47 g, 3.50 mmol, 1.4 equivs), then was stirred overnight (15 h) at room temperature under nitrogen. The reaction was subsequently diluted with  $CH_2Cl_2$  (20 mL), washed with brine, and back-extracted with  $CH_2Cl_2$ . The combined organic layers were dried over  $Na_2SO_4$  and concentrated under reduced pressure, and the residue was flash column chromatographed on silica gel (heptane:EtOAc, 6:1), affording dipeptide **12** as a colorless oil (0.92 g; 55%);  $R_F$  0.69 (heptane:EtOAc, 2:1);  $^1H$  NMR (250 MHz,  $CDCl_3$ )  $\delta$  -0.25, -0.23, -0.01, 0.16 (s, 3H), 0.71, 1.01 (s, 9H), 1.39 (s, 9H), 3.49 (s, 3H), 4.22 (d,  $J = 2.0$  Hz, 1H), 4.39 (d,  $J = 3.1$  Hz, 1H), 5.01 (dd,  $J = 3.3, 9.6$  Hz, 1H), 5.11 (d,  $J = 7.4$  Hz, 1H), 6.28 (d,  $J = 9.4$  Hz, 1H), 7.22-7.29 (m, 10H), 7.52 (d,  $J = 7.0$  Hz, 1H);  $^{13}C$  NMR (50.32 MHz,  $CDCl_3$ )  $\delta$  -5.73, -5.18, -4.94, -3.51, 18.00, 18.35, 25.48, 26.03, 28.41, 52.17, 56.47, 57.16, 75.45, 79.34, 126.85, 127.30, 127.72, 128.15, 128.33, 138.54, 138.95, 155.03, 171.38; MS (CI, isobutane, 180  $^\circ C$ ) 687 [M + H], 510 ([M + 57]-Boc-TBSOH), 454 ([M + H]-TBSOH-Boc), 410 ([M + H] - monomer), 354 ([410]-t-Bu);  $[\alpha]_D^{20} + 17.9^\circ$  ( $c = 0.38$ ,  $CH_2Cl_2$ ); Anal. calcd for  $C_{36}H_{58}N_2O_7Si_2$ : C, 62.94; H, 8.52; N, 4.08. Found: C, 62.86; H, 8.48; N, 4.03.

**Boc-Tripeptide-OMe (13).** As for **10**, Boc-dipeptide-OMe **12** was stirred for 5 h at room temperature under nitrogen in a 1:1 v:v mixture of  $CH_2Cl_2$  and formic acid (20 mL). The resulting *N*-deprotected dipeptide methyl ester-HCO<sub>2</sub>H (white solid) (0.83 g, 1.31 mmol) and potassium *N*-tert-butoxycarbonyl-*O*-tert-butylidimethylsilylphenylisoserinate **11** (1.12 g, 2.62 mmol, 2 equivs) were reacted in the presence of Pybop (1.36 g, 2.62 mmol, 2 equivs), NMM (0.58 mL, 5.24 mmol, 4 equivs) and HOBt (354 mg, 2.62 mmol, 2 equivs). Tripeptide **13** was obtained as a white solid (1.08 g; 86%) after flash column chromatography on silica gel (heptane:EtOAc, 10:1);  $R_F$  0.77 (1:1, heptane:EtOAc);  $^1H$  NMR (250 MHz,  $CDCl_3$ )  $\delta$  -0.16 (s, 6H), -0.08, 0.01, 0.17, 0.28 (s, 3H), 0.75, 0.93, 0.99 (s, 9H), 1.33 (s, 9H), 3.28 (s, 3H), 3.71 (d,  $J = 3.9$  Hz, 1H), 3.98 (d,  $J = 2.7$  Hz, 1H), 4.34 (d,  $J = 2.7$  Hz, 1H), 5.01 (m,  $J = 2$  Hz, 1H), 5.13 (dd,  $J = 2.4, 9.0$  Hz, 1H), 6.22 (d,  $J = 9.4$  Hz, 1H), 7.14-7.33 (m, 15H), 7.39 (d,  $J = 8.6$  Hz, 1H), 8.37 (d,  $J = 9.0$  Hz, 1H);  $^{13}C$  NMR (62.89 MHz,  $CDCl_3$ )  $\delta$  -5.52, -5.27, -5.06, -4.53, -3.46, 17.97, 18.30, 25.56, 25.92 ( $\times 2$ ), 28.40, 51.78, 55.11 ( $\times 2$ ), 57.35, 73.62, 75.16, 76.33, 79.24, 127.00, 127.22, 127.49, 127.60, 128.06, 128.12, 137.16, 138.33, 138.98, 155.11, 170.54, 170.72, 171.15; MS (CI, isobutane, 210  $^\circ C$ ) 964 ([M + H]), 864 ([M + H] - Boc), 687 ([M + H] - monomer), 410 ([monomer + H]);

(27) The yield of **9** after chromatography exceeds 100% due to the presence of TBSOH. This contaminant was removed by prolonged drying under vacuum with slight heating (30-40  $^\circ C$ ).



$[\alpha]_D^{20} +19.1^\circ$  ( $c = 0.86$ ,  $\text{CH}_2\text{Cl}_2$ ); Anal. calcd for  $\text{C}_{51}\text{H}_{81}\text{N}_3\text{O}_9\text{Si}_3$ : C, 63.52; H, 8.47; N, 4.36. Found: C, 63.43; H, 8.39; N, 4.19.

**H-Triptide-OMe (Formate Salt) (14).** As for **10**, Boc-tripeptide-OMe **13** (0.52 g, 0.54 mmol) was stirred for 4 h at room temperature under nitrogen in a 1:1 v:v mixture of  $\text{CH}_2\text{Cl}_2$  and formic acid (30 mL). The solvent was then evaporated, and the residue was dried under vacuum until a solid was obtained. The resulting solid was washed with a small amount of ether and dried under vacuum, giving *N*-deprotected tripeptide methyl ester— $\text{HCO}_2\text{H}$  **14** as a white solid (0.49 g; 100%).  $^1\text{H}$  NMR (250 MHz,  $\text{CDCl}_3$ )  $\delta$  -0.49, -0.21, -0.20, -0.19, 0.19, 0.26 (s, 3H), 0.72, 0.83, 0.98 (s, 9H), 3.35 (s, 3H), 4.09 (d,  $J = 4.0$  Hz, 1H), 4.25 (d,  $J = 4.2$  Hz, 1H), 4.32 (d,  $J = 4.6$  Hz, 1H), 4.38 (s, 1H), 5.14–5.25 (m, 2H), 7.14–7.33 (m, 17H), 7.47 (d,  $J = 9.3$  Hz, 1H), 8.18 (d,  $J = 9.3$  Hz, 1H).

**Boc-Tripeptide-OH (Potassium Salt) (15).** *Method A.* To a solution of Boc-tripeptide-OMe **13** (0.44 g, 0.46 mmol) in dry ether (20 mL) was added potassium trimethylsilylanolate (0.29 g, 2.28 mmol, 5 equivs) in 3 portions over 2 h intervals, and the mixture was stirred under nitrogen at room temperature for 5 h and then at refluxed for 2 h. The solvent was then evaporated, and the residue was washed with heptane: ether (3:1). After drying under vacuum, compound **15** was carried on to the next coupling step without further purification.

*Method B.* To a solution of Boc-tripeptide-OMe **13** (151 mg, 0.16 mmol) in dry ether (15 mL) was added potassium trimethylsilylanolate (0.022 g, 0.17 mmol, 1.1 equivs), and the mixture was stirred under nitrogen for 4 h at room temperature before adding an additional 0.5 equiv of TMSOK and stirring for another 5 h. The solvent was then evaporated, and the residue was washed with heptane—ether (3:1). After drying under vacuum, compound **15** was carried on to the next coupling step without further purification.

**Boc-Tetrapeptide-OMe (16).** As for **12**, the formate salt of H-tripeptide-OMe **14** (236 mg, 0.26 mmol) and potassium *N*-tert-butoxycarbonyl-*O*-tert-butylidimethylsilylphenylisoserinate **11** (338 mg, 0.78 mmol, 3 equivs) were reacted in the presence of Pybop (406 mg, 0.78 mmol, 3 equivs), NMM (86  $\mu\text{L}$ , 0.78 mmol, 3 equivs) and HOBt (105 mg, 0.78 mmol, 3 equivs). Tetrapeptide **16** was obtained as a white solid (277 mg, 86%) after flash column chromatography on silica gel (heptane:EtOAc, 6:1):  $R_f$  0.49 (2:1, heptane:EtOAc);  $^1\text{H}$  NMR (250 MHz,  $\text{CDCl}_3$ )  $\delta$  -0.26, -0.18, -0.17 (s, 3H), -0.04 (s, 6H), 0.01, 0.11, 0.13, 0.24 (s, 3H), 0.73, 0.79, 0.99, 1.01 (s, 9H), 1.32 (s, 9H), 3.25 (s, 3H), 3.29 (d,  $J = 3.9$  Hz, 1H), 3.80 (d,  $J = 3.9$  Hz, 1H), 3.88 (d,  $J = 2.3$  Hz, 1H), 4.39 (d,  $J = 2.7$  Hz, 1H), 4.94–5.05 (m, 4H), 6.31 (d,  $J = 9.0$  Hz, 1H), 7.02–7.53 (m, 20H), 8.07 (d,  $J = 8.2$  Hz, 1H), 8.25 (d,  $J = 9.8$  Hz, 1H), 8.34 (d,  $J = 9.4$  Hz, 1H);  $^{13}\text{C}$  NMR (62.89 MHz,  $\text{CDCl}_3$ )  $\delta$  -5.89, -5.46, -5.01, -4.54, 17.97, 18.18, 18.29, 19.31, 25.57, 25.97, 26.08, 28.47, 51.76, 54.09, 54.82, 55.09, 57.59, 73.86, 74.39, 75.08, 76.17, 78.08, 78.41, 80.66, 120.51, 125.05, 126.66, 127.03, 127.13, 127.33, 127.48, 127.82, 127.97, 128.08, 128.18, 128.85, 137.06, 137.25, 138.40, 139.15, 155.22, 170.06, 170.38, 170.85, 171.20; MS (FAB, 500  $^\circ\text{C}$ ): 1241.6 ([M + H]), 1141.6 ([M + H] - Boc), 1036.5, 864.5;  $[\alpha]_D^{20} +37.0^\circ$  ( $c = 0.40$ ,  $\text{CH}_2\text{Cl}_2$ ).

**Boc-Pentapeptide-OMe (17).** Boc-Tetrapeptide-OMe **16** (260 mg, 0.21 mmol) was stirred for 3 h at room temperature under nitrogen in a 1:1 v:v mixture of  $\text{CH}_2\text{Cl}_2$  and formic acid (20 mL). The solvent was then evaporated, and the residue was dried under vacuum until a solid was obtained. The resulting solid was washed with a small amount of ether and dried under vacuum, giving the corresponding *N*-deprotected tetrapeptide methyl ester— $\text{HCO}_2\text{H}$  as a white solid (249 mg; 100%). As for **12**, this intermediate (249 mg, 0.21 mmol) and potassium *N*-tert-butoxycarbonyl-*O*-tert-butylidimethylsilylphenylisoserinate **11** (338 mg, 0.78 mmol, 3.7 equivs) were reacted in the presence of Pybop (406 mg, 0.78 mmol, 3.7 equivs), NMM (86  $\mu\text{L}$ , 0.78 mmol, 3.7 equivs) and HOBt (105 mg, 0.78 mmol, 3.7 equivs). Pentapeptide **17** was obtained as a white solid (185 mg, 58%) after flash column chromatography on silica gel (heptane:EtOAc, 5:1):  $R_f$  0.66 (2:1, heptane:EtOAc);  $^1\text{H}$  NMR (250 MHz,  $\text{CDCl}_3$ )  $\delta$  -0.19, -0.16, -0.10, 0.05, 0.08, 0.11, 0.18, 0.19, 0.20, 0.29 (s, 3H), 0.72, 0.97, 0.98, 0.99, 1.06 (s, 9H), 1.30 (s, 9H), 3.07 (d,  $J = 3.5$  Hz, 1H), 3.24 (s, 3H), 3.46 (d,  $J = 3.5$  Hz, 1H), 3.88 (m, 2H), 4.38 (d,  $J = 2.7$  Hz, 1H), 4.91 (dd,  $J = 3.5$ , 9.8 Hz, 1H), 5.00–5.11 (m, 4H), 6.30 (d,  $J = 9.0$  Hz, 1H), 7.00 (m, 3H), 7.13–7.42 (m, 23H), 8.12 (d,  $J = 10.6$  Hz, 1H), 8.22 (d,

$J = 9.8$  Hz, 1H), 8.40 (d,  $J = 9.4$  Hz, 1H);  $^{13}\text{C}$  NMR (62.89 MHz,  $\text{CDCl}_3$ )  $\delta$  -5.57, -5.41, -5.32, -5.14, -4.90, -4.69, -4.47, -3.50, 17.86, 18.10, 18.19, 25.27, 25.51, 25.75, 25.89, 25.94, 28.35, 51.67, 53.55, 53.89, 54.72, 55.05, 57.56, 73.87, 74.06, 74.53, 75.14, 76.26, 77.48, 79.18, 83.39, 126.93, 127.02, 127.16, 127.33, 127.65, 127.78, 127.99, 128.26, 134.06, 136.98, 137.16, 138.46, 139.07, 155.14, 169.94 ( $\times 2$ ), 170.17, 170.75, 171.09; MS (FAB, 500  $^\circ\text{C}$ ): 1518.7 ([M + H]), 1419.7, 1418.7 ([M + H] - Boc), 1313.6, 1242.6, 1141.6;  $[\alpha]_D^{20} +95.0^\circ$  ( $c = 0.02$ ,  $\text{CH}_2\text{Cl}_2$ ).

**Boc-Hexapeptide-OMe (18).** *Tripeptide Coupling (14 + 15).* As for dipeptide **12**, H-tripeptide-OMe ( $\text{HCO}_2\text{H}$ ) **14** (136 mg, 0.15 mmol) and the *O*-deprotected tripeptide **15** (potassium salt) (158 mg, 0.16 mmol, 1.1 equivs) were reacted in the presence of Pybop (125 mg, 0.24 mmol, 1.6 equivs), NMM (53  $\mu\text{L}$ , 0.48 mmol, 3.2 equivs), and HOBt (32 mg, 0.24 mmol, 1.6 equivs). Hexapeptide **18** was obtained as a white solid (107 mg, 40%) after flash column chromatography on silica gel (heptane:EtOAc, 10:1):

**Linear Approach (17 + 11).** Boc-pentapeptide-OMe **17** (180 mg, 0.12 mmol) was stirred for 3 h at room temperature under nitrogen in a 1:1 v:v mixture of  $\text{CH}_2\text{Cl}_2$  and formic acid (20 mL). The solvent was then evaporated, and the residue was dried under vacuum until a solid was obtained. The resulting solid was washed with a small amount of ether and dried under vacuum, giving the corresponding *N*-deprotected pentapeptide methyl ester— $\text{HCO}_2\text{H}$  as a white solid (176 mg; 100%). As for dipeptide **12**, this intermediate (176 mg, 0.12 mmol) and potassium *N*-tert-butoxycarbonyl-*O*-tert-butylidimethylsilylphenylisoserinate **11** (338 mg, 0.78 mmol, 6.5 equivs) were reacted in the presence of Pybop (406 mg, 0.78 mmol, 6.5 equivs), NMM (86  $\mu\text{L}$ , 0.78 mmol, 6.5 equivs), and HOBt (105 mg, 0.78 mmol, 6.5 equivs). Hexapeptide **18** was obtained as a white solid (107 mg, 50%) after flash column chromatography on silica gel (heptane:EtOAc, 8:1):  $R_f$  0.59 (2:1, heptane:EtOAc). In certain instances preparative HPLC was alternatively used to purify **18** [C18 column (10 mm  $\times$  250 mm);  $\text{CH}_3\text{-CN}:\text{EtOAc}$ , 80–20; elution rate, 6 mL/min; elution time, 19 min];  $^1\text{H}$  NMR (250 MHz,  $\text{CDCl}_3$ )  $\delta$  -0.21, -0.20, -0.07, 0.03 (s, 3H), 0.07 (s, 6H), 0.11 (s, 3H), 0.15 (s, 6H), 0.16, 0.24, 0.26 (s, 3H), 0.72 (s, 9H), 0.96 (s, 18H), 0.99, 1.02, 1.05 (s, 9H), 1.31 (s, 9H), 2.99 (d,  $J = 3.9$  Hz, 1H), 3.24 (s, 3H), 3.24 (d,  $J = J$  Hz, 1H), 3.45 (d,  $J = 3.5$  Hz, 1H), 3.83 (d,  $J = 3.9$  Hz, 1H), 3.87 (d,  $J = 2.3$  Hz, 1H), 4.38 (d,  $J = 2.7$  Hz, 1H), 4.87 (dd,  $J = 3.5$ , 10.2 Hz, 1H), 4.95–5.10 (m, 5H), 6.31 (d,  $J = 9.4$  Hz, 1H), 6.98 (m, 3H), 7.09–7.35 (m, 28H), 8.03 (d,  $J = 12.1$  Hz, 1H), 8.07 (d,  $J = 10.6$  Hz, 1H), 8.27 (d,  $J = 9.8$  Hz, 1H), 8.40 (d,  $J = 9.4$  Hz, 1H);  $^{13}\text{C}$  NMR (50.32 MHz,  $\text{CDCl}_3$ )  $\delta$  -5.51, -5.18, -5.06, -4.70, -4.57, 17.94, 18.17, 18.28, 25.57, 25.96 ( $\times 2$ ), 28.42, 51.74, 53.48, 54.04, 54.78, 55.14, 57.39, 57.60, 73.66, 73.82, 73.99, 74.27, 74.71, 75.19, 79.28, 127.03, 127.28, 127.57, 127.65, 127.80, 127.91, 128.04, 128.16, 137.06, 137.24, 138.53, 139.04, 155.19, 169.84, 169.98, 170.22, 170.80, 171.17; MS (FAB, 500  $^\circ\text{C}$ ): 1796.7, 1795.7 ([M + H]), 1696.7 ([M + H] - Boc), 1682.7, 1639.6; UV-vis ( $c = 0.014$  mM,  $\text{CHCl}_3$ )  $\lambda_{\text{max}}$  294 nm ( $\epsilon = 3.2 \times 10^4$   $\text{L mol}^{-1}$   $\text{cm}^{-1}$ );  $[\alpha]_D^{20} +31.4^\circ$  ( $c = 0.87$ ,  $\text{CH}_2\text{Cl}_2$ ); Anal. calcd for  $\text{C}_{96}\text{H}_{150}\text{O}_{15}\text{N}_6\text{Si}_6$ : C, 64.18; H, 8.42; N, 4.68. Found: C, 64.27; H, 8.45; N, 4.47%.

**CD of Hexa- $\beta$ -peptide (18).** The CD spectrum was recorded from 190 to 280 nm on a JASCO J-710 dichrograph equipped with a thermostatically controlled cell holder and connected to a computer for data acquisition. For a 0.1 nM solution of **18** dissolved in chloroform the data were collected at 20  $^\circ\text{C}$  using cells with a 1-mm path length.

**NMR of Hexa- $\beta$ -peptide (18).** 1D  $^1\text{H}$  NMR (500 MHz): 16 K data points, 32 scans, 1.365-s acquisition time.

2D NMR DQCOSY: Acquisition: 4 K ( $t_2$ )  $\times$  350 ( $t_1$ ) data points; 32 scans per  $t_1$  increment; 0.341-s acquisition time in  $t_2$ ; max acquisition time in  $t_1$ , 0.0583 s; relaxation delay, 2 s; states quadrature detection in  $\omega_1$ . Processing: zero filling and Ft to  $2\text{K} \times 1\text{K}$  real data points after multiplication with sin filter shifted by  $\pi/4$  in  $\omega_2$  and sin filter in  $\omega_1$ .

Clean-TOCSY (MLEV16 with Spin Lock Power of 11 kHz): Acquisition: 4 K ( $t_2$ )  $\times$  350 ( $t_1$ ) data points; 64 scans per  $t_1$  increment; 0.341-s acquisition time in  $t_2$ ; max acquisition time in  $t_1$ , 0.0583 s; mixing time, 40 ms; states quadrature detection in  $\omega_1$ . Processing: zero filling and Ft to  $2\text{K} \times 1\text{K}$  real data points after multiplication with sin filter shifted by  $\pi/3$  in  $\omega_2$  and sin filter in  $\omega_1$ .

**HSQC:** Acquisition: 2 K (t2)  $\times$  400 (t1) data points; 32 scans per t1 increment; 0.171-s acquisition time in t2; max acquisition time in t1, 0.0412 s; states quadrature detection in  $\omega_1$ . Processing: zero filling and Ft to 1K  $\times$  1K real data points after multiplication with Gaussian filter (gf = 0.072 s, gfs = 0.025 s) in  $\omega_2$ , and  $\sin^2$  filter shifted by  $\pi/4$  in  $\omega_1$ .

**HMBC:** Acquisition: 4 K (t2)  $\times$  512 (t1) data points; 96 scans per t1 increment; 0.341-s acquisition time in t2; max acquisition time in t1, 0.0455 s; no  $^{13}\text{C}$  decoupling. Processing: zero filling and Ft to 2K  $\times$  2K real/real data points after multiplication by sin filter shifted by  $\pi/4$  in  $\omega_2$ , and sin filter in  $\omega_1$ .

**ROESY:** a series of 3 ROESY spectra with mixing time of 100, 200, and 400 ms was acquired with spin-lock pulse with effective field of 6.2 kHz. Acquisition: 4 K (t2)  $\times$  350 (t1) data points; 64 scans per t1 increment; 0.341-s acquisition time in t2; max acquisition time in t1, 0.0583 s; states quadrature detection in  $\omega_1$ . Processing: zero filling and Ft to 2K  $\times$  1K real/real data points after multiplication by  $\sin^2$  filter shifted by  $\pi/5$  in  $\omega_2$ , and sin filter shifted by  $\pi/5$  in  $\omega_1$ .

**Structure Determination.** Model-building and molecular dynamics simulations were performed on a SGI Indigo workstation in the context of the Insight/Discover molecular modeling package (Molecular

Simulations, Inc.). The calculation began with energy minimization steps on the starting structure with only the covalent constraints using a quartic potential and very low force constants for each term of the pseudo-energy function ( $\times 10^{-6}$ ). Restrained dynamics were then carried out by heating the system to 1000 K. Distance, angle, and chirality constraints were included, and the force constants were scaled up during these steps. Then the system was cooled to 300 K while maintaining the constraints force constants to their full value. The final structures were obtained after a last restraint energy minimization step with other parameters left unchanged.

**Acknowledgment.** We thank Rhone-Poulenc Rorer, Vitry-sur-Seine, France (Aventis) for a generous gift of (–)-(2*R*, 3*S*)-phenylisoserine.

**Supporting Information Available:** Chirality, distance, and angle constraints used to calculate the structure of homo- $\beta$ -peptide **18** and amide proton exchange studies. This material is available free of charge via the Internet at <http://pubs.acs.org>.

JA002700+